Biogeosciences
Open Access
Discussions

Fukushima-derived radiocesium in western North Pacific sediment traps

M. C. Honda[1], H. Kawakami[2], S. Watanabe[2], and T. Saino[1]

[1]Research Institute for Global Change, Japan Agency for Marine-Earth Science and Technology, 2-15 Natsushima, Yokosuka, Kanagawa 237-0061, Japan
[2]Mutsu Institute for Oceanography, Japan Agency for Marine-Earth Science and Technology, 690 Aza-kitasekine, Oaza-sekine, Mutsu, Aomori 035-0022, Japan

Correspondence to: M. C. Honda (hondam@jamstec.go.jp)

Discussion Paper | Discussion Paper | Discussion Paper | Discussion Paper

BGD

10, 2455–2477, 2013

Fukushima-derived radiocesium in western North Pacific sediment traps

M. C. Honda et al.

Title Page

Abstract	Introduction
Conclusions	References
Tables	Figures

|◄ | ►|
◄ | ►

Back | Close

Full Screen / Esc

Printer-friendly Version

Interactive Discussion

Abstract

At two stations in the western North Pacific, K2 in the subarctic gyre and S1 in the subtropical gyre, time-series sediment traps were collecting sinking particles when the Fukushima Daiichi Nuclear Power Plant (FNPP1) accident occurred on 11 March 2011. Radiocesium (^{134}Cs and ^{137}Cs) derived from FNPP1 accident was detected in sinking particles collected at 500 m by late March 2011 and at 4810 m by early April 2011 at both stations. The sinking velocity of ^{134}Cs and ^{137}Cs was estimated to be 8 to 36 m day^{-1} between the surface and 500 m and > 180 m day^{-1} between 500 m and 4810 m. ^{137}Cs specific activity varied from 0.14 to 0.25 Bq g^{-1} dry weight. These values are higher than those of surface seawater, suspended particles, and zooplankton collected in April 2011. Although the radiocesium may have been adsorbed onto or incorporated into clay minerals, correlations between ^{134}Cs and lithogenic material were not always significant; therefore, the form of the cesium associated with the sinking particles is still an open question. The total ^{137}Cs flux by late June at K2 and by late July at S1 was 0.5 to 1.7 Bq m^{-2} at both depths. Compared with ^{137}Cs input to both stations by April 2011, estimated from the surface ^{137}Cs activity and mixed layer depth and by assuming that the observed ^{137}Cs flux was constant throughout the year, the estimated removal rate of ^{137}Cs from the upper layer (residence time in the upper layer) was 0.3 to 1.5 % (68 to 312 yr). The estimated removal rates and residence times are comparable to previously reported values.

1 Introduction

On 11 March 2011, the 2011 Tohoku-Oki Earthquake of magnitude 9.0 occurred off Miyagi Prefecture, Japan. This earthquake and the tsunami it generated seriously damaged the Fukushima Daiichi Nuclear Power Plant (FNPP1). As a result of the loss of power and the associated malfunction of the cooling system, large quantities of artificial radionuclides were emitted from FNPP1 by hydrogen explosions, venting, and

intentional and accidental discharge of radiologically contaminated water. An estimated 15 PBq of ^{137}Cs was emitted by hydrogen explosions and intentional venting (Chino et al., 2011; NERH, 2011). This amount corresponds to about one-sixth of the quantity released by the Chernobyl nuclear power plant (CNPP) accident in 1986 (85 PBq; WHO 1989). Morino et al. (2011) reported that only about 22 % of the ^{137}Cs released from FNPP1 was deposited on land in March 2011. Thus, one of the big differences between the FNPP1 accident and the CNPP accident is that, because FNPP1 is in a coastal area, most of the released radionuclides (about 80 % of total emissions) were deposited in the ocean. Direct discharge of ^{137}Cs in contaminated water was estimated to be 3.5–5.9 PBq (Kawamura et al., 2011; Tsumune et al., 2011; Miyazawa et al., 2012). In addition, eolian input of ^{137}Cs was estimated to be 5 to 10 PBq (Kawamura et al., 2011; Miyazawa et al., 2012; Aoyama et al., 2013). About one month after the FNPP1 accident, Honda et al. (2012) investigated the dispersion of FNPP1-derived radiocesium in the western North Pacific. They measured radiocesium in surface water, suspended particles, and zooplankton and performed a mathematical simulation that verified that FNPP1-derived radiocesium had dispersed over a broad area of the western North Pacific. They suspected that radiocesium detected in remote parts of the North Pacific had been transported via the atmosphere and was not derived from the released contaminated water. Since then the dispersion of FNPP1-derived radionuclides has been investigated over an even broader area by voluntary observing ships and scientific cruises (Aoyama et al., 2012; Buesseler et al., 2012) and by mathematical simulations (Masumoto et al., 2012; Miyazawa et al., 2012). Nevertheless, the vertical invasion and transport of radionuclides in the ocean is still insufficiently understood. Radionuclides invade the ocean interior by vertical diffusion and advection or on sinking particles. After the CNPP accident, radionuclides on sinking particles were collected by sediment traps in the Black Sea (Buesseler et al., 1987, 1990), North Sea (Kempe and Nies, 1987), Mediterranean Sea (Fowler et al., 1987), and North Pacific (Kusakabe et al., 1988), and the arrival dates of the CNPP-derived radionuclides at the

Fukushima-derived radiocesium in western North Pacific sediment traps

M. C. Honda et al.

different stations as well as the sinking velocity and removal rate of the particles were determined.

At the time of the FNPP1 accident, sediment traps had already been deployed at time-series stations in the northwestern North Pacific to collect sinking particles for studies of biogeochemical cycling and how it would be affected by climate and oceanic change (project URL: http://www.jamstec.go.jp/rigc/e/ebcrp/mbcrt/index.html). Here, we document the specific activity and flux of FNPP1-derived radiocesium, [134]Cs (half life, 2.06 yr) and [137]Cs (half life, 30.17 yr), in sinking particles collected at these stations before and after the FNPP1 accident. Then, we estimate the sinking velocity of the particles and discuss the form and particle scavenging process of the radiocesium.

2 Method

2.1 Sediment trap positions

In November 2010, time-series sediment traps (McLane Mark7G-21) were deployed at 500 m and 4810 m at stations K2 (47° N, 160° E; water depth, $\sim$5200 m), which is in the subarctic gyre, and S1 (30° N, 145° E; water depth, $\sim$5800 m), which is in the subtropical gyre (Fig. 1). The horizontal distances from FNPP1 to K2 and S1 are about 1870 km and 950 km, respectively. Before the traps were deployed, their collecting cups were filled with a seawater-based 10 % buffered formalin solution as a preservative. The sampling interval was 12 days. The sediment traps at K2 and S1 were recovered in June and July 2011, respectively, by R/V *Mirai*.

2.2 Chemical analysis

In the laboratory, sediment trap samples were sieved through a 1 mm plastic mesh to eliminate zooplankton "swimmers". The samples were then divided into 10 or more fractions by using a McLane splitter. Some fractions were rinsed with a small amount of distilled water through pre-weighed Nuclepore filters (0.4 µm pore size) and dried

Fukushima-derived radiocesium in western North Pacific sediment traps

M. C. Honda et al.

at 50 °C for 24 h. The dried samples were then weighed and total mass fluxes were computed. Subsequently, the samples were scraped off the filters and pulverized with an agate mortar.

For measurement of the total carbon concentration (TC), samples of about 5 mg were precisely weighed in a tin capsule. Samples for the measurement of organic carbon (OC) were precisely weighed on GF/F filters, and then the GF/F filters with sample were placed in a container filled with HCl mist for 24 h to eliminate $CaCO_3$. After decalcification, the filter with sample was wrapped in a tin disk. Samples in the tin capsule or wrapped in the tin disk were placed in the auto-sampler of an elemental analyzer (Perkin-Elmer 2400), and TC, OC and the concentration of nitrogen (N) were measured. The concentration of inorganic carbon (IC) was determined as the difference between TC and OC. Measurement errors were mainly less than 3 %.

For measurement of trace elements, samples of about 20 mg were precisely weighed in a graphite crucible. About 140 mg of lithium metaborate ($LiBO_4$) (approximately seven times the sample mass) was then added and mixed well with the sample. Samples in graphite crucibles were placed in a furnace and maintained for 15 min at 950 °C. The resulting "lava-like" samples were placed in a Teflon beaker with 6 % nitric acid solution (HNO_3, ~ 20 mL) and stirred for 1 h. This solution was filtered through a GF/F filter to eliminate graphite debris, its volume was adjusted to 50 mL by adding 6 % HNO_3 solution, and then it was weighed precisely. Concentrations of trace elements (Si, Ca, Fe, Ti, Mn, Mg, Ba, K) were measured by ICP-AES (Perkin-Elmer Optima 3300DV). Measurement errors were less than 5 % for every element. Concentrations of organic materials (OM), $CaCO_3$, biogenic opal and lithogenic material (LM) were calculated following Honda et al. (2002).

Specific activities of [134]Cs and [137]Cs (hereinafter activities) were measured in samples collected after 1 March 2012. A plastic tube was filled with dried and pulverized samples, and the specific gamma rays emitted by [134]Cs and ^{137}Cs were measured by gamma spectrometry with a well-type Ge detector (ORTEC GWL-120210). The Ge detector was calibrated by using mixed-volume sources (Eckert & Ziegler Isotope

Products, EG-ML). The counting time varied from one day to a few days. The [134]Cs activity was corrected for cascade summing (43–49 %). The detection limit was 10 mBq per sample. Concentrations of radiocesium were decay-corrected to the date and time of the middle day of the sampling period. The precision of [134]Cs and ^{137}Cs measurements was one sigma of the counting error.

3   Results

3.1   Seasonal variability of the flux and chemical composition of sinking particles

3.1.1   K2

The total mass flux (TMF) of sinking particles at 500 m at K2 (K2-500 m) decreased from November 2010 to February 2011 (Fig. 2a). After the FNPP1 accident in March 2011, TMF increased and, although it dipped in early May, the highest value was reached in June. In autumn and winter, $CaCO_3$ was the dominant component of the samples, whereas biogenic opal was dominant after March. During the entire observation period, biogenic opal and $CaCO_3$ concentrations were estimated to average 47 % and 31 %, respectively. At K2-4810 m, the TMF was not as large as at 500 m, but its seasonal variability was similar; it decreased from November 2010 and mainly increased, with low values in May, from March to June 2011 (Fig. 2b). The LM concentration was relatively higher (24 %) at 4810 m than at 500 m (6 %). We attribute this result to LM being more refractory than biogenic materials. Biogenic opal accounted for about 33 % of each sample, and was also dominant in the annual average. Therefore, the sediment trap samples from K2 used for the radiocesium analysis in this study consisted of sinking particles, of which biogenic opal was the major component, and the TMF tended to increase from March toward early summer.

3.1.2 S1

The smallest TMF was observed at S1-500 m at the time that the sediment trap was deployed in November 2010 (Fig. 2c). It began to increase in late December 2010 and reached a maximum in January 2011, after which it decreased before rising again in March 2011. Thereafter, TMF tended to decrease toward July 2011. The $CaCO_3$ concentration was about 80 % on average, and $CaCO_3$ was the major component of sinking particles. At S1-4810 m, TMF also increased from late December 2010 to January 2011 (Fig. 2d), and TMF peaks were observed in March and late April 2011. In general, the seasonal variability at 4810 m was similar to that at 500 m. Although concentrations of biogenic opal and LM in the samples were higher at 4810 m than at 500 m, $CaCO_3$ was still the dominant component at 4810 m. Therefore, samples for radiocesium analysis from S1 consisted of sinking particles whose major component was $CaCO_3$, and the TMF tended to gradually decrease from March toward June.

3.2 Activity and flux of radiocesium

The activities and fluxes of ^{134}Cs and ^{137}Cs are listed in Table 1 and shown against time in Fig. 3. ^{134}Cs was detected in almost all samples, whereas before the FNPP1 accident, ^{134}Cs activity was zero worldwide (e.g. Aoyama and Hirose, 2004). In addition, in all samples the ratio of ^{134}Cs to ^{137}Cs (^{134}Cs/^{137}Cs) was about one, which was the ratio in the radionuclides released by the FNPP1 accident, as verified by radiocesium analysis of seawater (Buesseler et al., 2011, 2012), aerosols (Haba et al., 2012) and soil (Qin et al., 2012). Thus, there is no doubt that the radiocesium detected in the sinking particles was derived from the FNPP1 accident.

3.2.1 K2

At K2-500 m, ^{134}Cs and ^{137}Cs were detected for the first time in sinking particles collected between 25 March and 6 April 2011 (Fig. 3a). The ^{134}Cs activity in this sample,

$0.48\,\mathrm{Bq\,g^{-1}}$, was the maximum among all sediment trap samples analyzed in this study. Subsequently, [134]Cs activity tended to decrease gradually. The largest [134]Cs flux was also observed between 25 March and 6 April ($36.2\,\mathrm{mBq\,m^{-2}\,day^{-1}}$), and it also tended to decrease thereafter.

At K2-4810 m, [134]Cs was initially detected in sinking particles collected during the next sampling interval, between 6 and 18 April, 12 days after it was first detected at K2-500 m (Fig. 3b). Unlike at K2-500 m, at K2-4810 m, [134]Cs activity increased over time, and it reached its largest value of $0.35\,\mathrm{Bq\,g^{-1}}$ between 24 May and 6 June 2011. No [134]Cs was detected in sinking particles collected between 12 and 24 May or between 17 and 29 June, probably because the sample mass was insufficient for detection by the gamma procedure rather than because the sinking particles contained no FNPP1-derived [134]Cs. At K2-4810 m, the [134]Cs flux was largest ($20.9\,\mathrm{mBq\,m^{-2}\,day^{-1}}$) between 5 and 17 June.

The average [134]Cs activity at K2-500 m and K2-4810 m during the observation period (500 m, 96 days; 4810 m, 60 days) was 0.27 and $0.19\,\mathrm{Bq\,g^{-1}}$, respectively. The total [134]Cs flux was $1.9\,\mathrm{Bq\,m^{-2}}$ at 500 m and $0.5\,\mathrm{Bq\,m^{-2}}$ at 4810 m (Table 2).

3.2.2   S1

At S1-500 m, [134]Cs was first detected in sinking particles collected between 25 March and 6 April, that is, the same period that they were first detected at K2-500 m (Fig. 3c). In general, [134]Cs activity tended to increase at S1-500 m, and it reached a maximum ($\sim 0.3\,\mathrm{Bq\,g^{-1}}$) in sinking particles collected between 17 and 29 June. As at K2-4810 m, and probably for the same reason, no [134]Cs was detected in sinking particle samples collected at S1-500 m between 6 and 18 April or between 24 May and 6 June. The [134]Cs flux was relatively higher in late April and June, and variations of the flux and the activity were generally synchronous. The total [134]Cs flux and average [134]Cs activity during the observation period (96 days) were estimated to be $0.5\,\mathrm{Bq\,m^{-2}}$ and $0.16\,\mathrm{Bq\,g^{-1}}$, respectively (Table 2).

At S1-4810 m ^{134}Cs was initially detected in sinking particles collected between 6 and 18 April (Fig. 3d), the same period that ^{134}Cs was first detected at K2-4810 m (Fig. 3b). ^{134}Cs activity increased toward late April and early May, and thereafter it fluctuated around a relatively constant value. A maximum ^{134}Cs activity of 0.25 Bq g^{-1} was de-tected in the sample collected between 17 and 29 June. The peak ^{134}Cs flux occurred between 30 April and 12 May, after which it decreased. The total ^{134}Cs flux and the average ^{134}Cs activity at S1-4810 m were estimated to be 1.0 Bq m^{-2} and 0.17 Bq g^{-1}, respectively (Table 2).

Previous ocean observations and mathematical simulation results suggest that the radiocesium detected at K2 and S1 in this study likely did not derive from contami-nated water discharged from FNPP1 and subsequently transported to the sediment trap station sites but from radiologically contaminated eolian dust (Honda et al., 2012).

4 Discussion

4.1 Sinking velocity

Although the distance to K2 from FNPP1 is double that to S1, it is noteworthy that at each respective depth FNPP1-derived radiocesium in sinking particles was first de-tected at both stations in the same period: at 500 m in samples collected between 25 March and 6 April, and at 4810 m in samples collected between 6 and 18 April. We estimated the sinking velocity of radiocesium between 500 m and 4810 m to be greater than $\sim$ 180 m day^{-1} [(4810 $-$ 500)/(12 + 12)]. This velocity is comparable to that esti-mated for sediment trap radionuclide data from the CNPP accident ($\sim$ 190 m day^{-1}: Kusakabe et al., 1988) and for general deep-sea sediment trap data ($\sim$ 140 m day^{-1}, Honda et al., 2009; 100–300 m day^{-1}, Berelson, 2002).

The results of a mathematical simulation of the transport of contaminated eolian dust containing radiocesium (Honda et al., 2012) suggest that eolian radiocesium ar-rived and was deposited at K2 on 14 March and at S1 on 18 March 2011. Under

the assumption that the eolian radiocesium arrived at 500 m between 26 March and 6 April, we estimated the sinking velocity between 0 (surface) and 500 m as 14 to 36 m day^{-1} at K2 and 8 to 20 m day^{-1} at S1. Although these values are smaller than the estimated general deep-sea sinking velocity of $\sim$ 140 m day^{-1}, these low velocities at shallow depth are comparable to the estimated radionuclide flux at shallow depth associated with the CNPP accident (> 20 m day^{-1} in the upper 1000 m of the Black Sea, Buesseler et al., 1987; 29 m day^{-1} in the upper 200 m of the Mediterranean Sea, Fowler et al., 1987; 65 ± 22 m day^{-1} in the upper 222 m of the North Sea, Kempe and Nies, 1987). This increase in the sinking velocity with depth is also supported by previous work (Berelson, 2002; Honda et al., 2009).

At K2-500 m, the sinking particles collected between 26 March and 18 April were composed of biogenic opal ($\sim$ 46 %) and CaCO$_3$ ($\sim$ 32 %,), whereas at S1-500 m, they consisted of $\sim$ 9 % biogenic opal and $\sim$ 72 % CaCO$_3$. Thus, at the two stations, the sinking velocities were comparable even though the chemical composition of the sinking particles differed.

4.2 Comparisons with radiocesium activities of sinking particles from the CNPP accident and those of seawater, suspended substances, and zooplankton

The ^{137}Cs activity of sinking particles observed this study ranged from 0.03 to 0.41 Bq g^{-1} (30–410 Bq kg^{-1}; Table 1). We estimated the average ^{137}Cs activity (total ^{137}Cs flux/TMF during the observation period) to be 0.18 to 0.25 Bq g^{-1} (180–250 Bq kg^{-1}) at K2 and 0.14 to 0.15 Bq kg^{-1} (140–150 Bq kg^{-1}) at S1 (Table 2). Compared with the ^{137}Cs activity resulting from the FNPP1 accident observed this study, the ^{137}Cs activities of sinking particles observed just after the CNPP accident were higher (Black Sea, 0.5 and 1.9 Bq g^{-1}, Buesseler et al., 1987; Mediterranean Sea, 0.15–4.0 Bq g^{-1}, Fowler et al., 1987; North Sea, 1.6–13.6 Bq g^{-1}, Kempe and Nies, 1987). The higher activities observed after the CNPP accident might be attributable to the fact that the amount of ^{137}Cs emitted during the CNPP accident was about six times the amount emitted during the FNPP1 accident. After the CNPP accident, the

Title Page

Abstract | Introduction

Conclusions | References

Tables | Figures

◀ | ▶

◀ | ▶

Back | Close

Full Screen / Esc

observed ^{137}Cs activities of surface seawater (Black Sea, 0.04–0.19 Bq kg^{-1}, Buesseler et al., 1987; North Sea, 0.07–0.3 Bq kg^{-1}, Kempe and Nies, 1987) were also higher than activities of surface seawater observed in April 2011 at K2 and S1 (0.009 and 0.018 Bq kg^{-1}, respectively), after the FNPP1 accident (Honda et al., 2012).

On the other hand, ^{137}Cs activities observed in sediment trap samples from the northern North Pacific and the Bering Sea after the CNPP accident (0.01–0.027 Bq g^{-1} in the North Pacific and 0.07–0.25 Bq g^{-1} in the Bering Sea, Kusakabe et al., 1987) were comparable to or smaller than those observed after the FNPP1 accident. These similar activities presumably reflect the fact that the distance between the CNPP and the North Pacific and Bering Sea sediment trap stations is about 8500 km, so the amount of ^{137}Cs transported from the CNPP to these areas was small.

In contrast to the relatively low ^{137}Cs activities of surface seawater at K2 and S1 in April 2011, about one month after the FNPP1 accident (Honda et al., 2012), ^{137}Cs activities of suspended particles in April 2011 at both stations were quite high, ranging from 3 to 32 Bq kg^{-1}, and activities of zooplankton collected at the same time ranged from 13 to 71 Bq kg^{-1} dry weight, slightly higher than those of suspended particles (Honda et al., 2012). These ^{137}Cs activities of zooplankton are comparable to both those of zooplankton observed after the CNPP accident in the Mediterranean Sea (Fowler et al., 1987) and those observed in the western North Pacific after the FNPP1 accident (Buesseler et al., 2011). However, ^{137}Cs activities of sinking particles this study (140–250 Bq kg^{-1} on average) were several times higher than those of zooplankton. Although the activities during the observation period were not steady-state values and only transient ^{137}Cs activity values of the various materials were measured, it is likely that the radiocesium associated with sinking particles was more refractory than that in living creatures.

Title Page

Abstract | Introduction

Conclusions | References

Tables | Figures

Back | Close

Full Screen / Esc

Printer-friendly Version

Interactive Discussion

4.3 Form of the radiocesium associated with sinking particles

Cesium, including radiocesium, is an alkaline metal that is regarded as soluble in water. The Chernobyl fallout was rapidly (within days) solubilized in seawater (Whitehead et al., 1988). However, a part of the cesium can be adsorbed onto or incorporated into aluminosilicates (clay minerals), similar to potassium (Qin et al., 2012, and references therein), and the adsorption or incorporation of cesium is not easily reversed (e.g. Kogure et al., 2012; Otosaka and Kobayashi, 2012). To determine the form of the radiocesium associated with sinking particles, we computed correlations between the concentration and flux of radiocesium with those of organic carbon, biogenic opal, $CaCO_3$, lithogenic materials (LM) and trace elements. We expected that radiocesium would correlate with LM or potassium, but the correlation between the ^{134}Cs flux and potassium or LM fluxes was not always significant. A possible reason for the failure to find a significant correlation is that the radiocesium concentrations and fluxes were transient values; consequently, the magnitude of radiocesium adsorption or incorporation might not be constant. Another possible reason is that some of the cesium was assimilated by living organisms (e.g. Kasamatsu and Ishikawa, 1997). Fowler et al. (1987) also reported that ^{137}Cs can become concentrated in fecal pellets. Moreover, Kaneyasu et al. (2012) reported that sulfate aerosol is a potential transport medium of radiocesium. Any of these circumstances could cause the correlation between radiocesium and potassium or LM to not be significant. Thus, the form of the radiocesium associated with sinking particles is still an open question. Precise measurements of stable Cs (^{133}Cs), electron microscopic analyses, and characterization/extraction experiments are needed to resolve this question.

4.4 Removal rate and residence time

In April 2011, ^{137}Cs activity of surface water was $0.009\,\mathrm{Bq\,kg^{-1}}$ at K2 and $0.018\,\mathrm{Bq\,kg^{-1}}$ at S1 (Honda et al., 2012), but Honda et al. (2012) did not detect radiocesium from FNPP1 in subsurface water (200 m). In April 2011, the surface mixed layer thickness

(SML) was 100 m at K2 and 60 m at S1. If it can be assumed that ^{137}Cs decreased linearly from the surface to the bottom of the SML, the ^{137}Cs inventory or input in April 2011 can be estimated as 450 Bq m^{-2} at K2 and 540 Bq m^{-2} at S1 (Table 2). The average ^{137}Cs flux to the ocean interior ranged from 7.6 to 18.1 mBq m^{-2} day^{-1} at K2 and from 4.7 to 8.0 mBq m^{-2} day^{-1} at S1 (Table 2). If these ^{137}Cs fluxes remained constant for a year, the removal rate at K2 can be estimated as 0.62 % yr^{-1} to 1.47 % yr^{-1} and the residence time as 68 to 161 yr, whereas the estimated removal rate at S1 is 0.32 % yr^{-1} to 0.54 % yr^{-1} and the estimated residence time is 184 to 312 years. From sediment trap and seawater ^{137}Cs data collected in the Black Sea in the several months following the CNPP accident, Buesseler et al. (1987) estimated a removal rate and residence time of radiocesium of 0.77 % yr^{-1} and 130 yr, respectively. Kusakabe et al. (1988) reported removal rates of 1 % in the North Pacific and Bering Sea for radiocesium from the CNPP accident, and Fowler et al. (1987) reported a removal rate of 0.2 % in the Mediterranean Sea. All of these removal rate estimates for radiocesium from the CNPP accident are comparable to our estimates for radiocesium from the FNPP1 accident. However, the ^{137}Cs concentration and flux might change with time, which might alter estimates of the removal rate and residence time. For example, using sediment trap data from an entire year, Buesseler et al. (1990) estimated a longer residence time (230–390 yr) in the Black Sea.

5 Concluding remarks and future work

Sediment trap data revealed that FNPP1-derived radiocesium was quickly transported to the deep sea in the western North Pacific. Estimates of the removal rate and residence time were comparable to previous estimates for CNPP-derived radiocesium. Moreover, data from sinking particles collected at K2 and S1 after the end of the observation period of this study confirm the increasing trend of TMF at K2 and the decreasing trend at S1 (Honda et al., 2013). In addition, except at K2-500 m, ^{134}Cs activity of sinking particles is continuing to increase. These new data will reveal more details about

the radiocesium flux associated with sinking particles. We also collected seafloor sediments at K2 and S1 in June/July 2011. The removal rate of radiocesium from the water column to the seafloor sediment and, conversely, its remobilization from sediments are also of considerable interest (e.g. Otosaka and Kobayashi, 2012). In addition, in July 2011 we deployed time-series sediment traps about 90 km off Fukushima, and data from these sediment traps will reveal not only the vertical transport of radiocesium to the ocean interior but also its lateral transport from the land or from shallower seafloor sediments.

References

Aoyama, M. and Hirose, K.: Artificial radionuclides database in the Pacific Ocean: HAM database, Sci. World J., 4, 200–215, 2004.

Aoyama, M., Tsumune, D., and Hamajima, Y.: Distribution of ^{137}Cs and ^{134}Cs in the North Pacific Ocean: impacts of the TEPCO Fukushima-Daiichi NPP accident, J. Radioanal. Nucl. Chem., doi:10.1007/s10967-012-2033-2, 2012.

Berelson, W. L.: Particle settling rates increase with depth in the ocean, Deep-Sea Res. Pt. II, 49, 237–251, 2002.

Buesseler, K. O., Livingston, H. D., Honjo, S., Hay, B. J., Manganini, S. J., Degens, E., Ittekkot, V., Izdar, E., Konuk, T., and Kempe, S.: Chernobyl radionuclides in a Black Sea sediment trap, Nature, 329, 825–828, 1987.

Buesseler, K. O., Livingston, H. D., Honjo, S., Hay, B. J., Konuk, T., and Kempe, S.: Scavenging and particle deposition in the southwestern Black Sea – evidence from Chernobyl radiotracers, Deep-Sea Res., 37, 413–430, 1990.

Buesseler, K. O., Aoyama, M., and Fukasawa, M.: Impacts of the Fukushima nuclear power plants on marine radioactivity, Environ. Sci. Tech., 45, 9931–9935, 2011.

Buesseler, K. O., Jayne, S. R., Fisher, N. S., Rypina, I. I., Baumann, H., Baumann, Z., Breier, C. F., Douglass, E. M., George, J., Macdonald, A. M., Miyamoto, H., Nishikawa, J., Pike, S. M., and Yoshida, S.: Fukushima-derived radionuclides in the ocean and biota off Japan, Proc. Natl. Acad. Sci., 109, 5984–5988, 2012.

Chino, M., Nakayama, H., Nagai, H., Terada, H., Katata, G., and Yamazawa, H.: Preliminary estimation of release amounts of ^{131}I and ^{137}Cs accidentally discharged from the Fukushima Daiichi nuclear power plant into the atmosphere, J. Nuclear Sci. Tech., 48, 1129–1134, 2011.

Fowler, S. W., Buat-Menard, P., Yokoyama, Y., Ballestra, S., Holm, E., and van Nguyen, H.: Rapid removal of Chernobyl fallout from Mediterranean surface waters by biological activity, Nature, 329, 56–58, 1987.

Haba, H., Kanaya, J., Mukai, H., Kambara, T., and Kase, M.: One-year monitoring of airborne radionuclides in Wako, Japan, after the Fukushima Daiichi nuclear power plant accident in 2011, Geochem. J., 46, 271–278, 2012.

Honda, M. C., Imai, K., Nojili, Y., Hoshi, F., Sugawara, T., and Kusakabe, M.: The biological pump in the northwestern North Pacific based on fluxes and major components of particulate matter obtained by sediment-trap experiment (1997–2000), Deep-Sea Res. Pt. II, 49, 5595–5625, 2002.

Honda, M. C., Sasaoka, K., Kawakami, H., Matsumoto, K., Watanabe, S., and Dickey, T.: Application of underwater optical data to estimation of primary productivity, Deep-Sea Res. Pt. I, 56, 2281–2292, 2009.

Honda, M. C., Aono, T., Aoyama, M., Hamajima, Y., Kawakami, H., Kitamura, M., Masumoto, Y., Miyazawa, Y., Takigawa, M., and Saino, T.: Dispersion of artificial caesium-134 and -137 in the western North Pacific one month after the Fukushima accident, Geochem. J., 46, e1–e9, 2012.

Kaneyasu, N., Ohashi, H., Suzuki, F., Okuda, T., and Ikemori, F.: Sulfate aerosol as a potential transport medium of radiocesium from the Fukushima nuclear accident, Environ. Sci. Tech., 46, 5720–5726, 2012.

Kasamatsu, F. and Ishikawa, Y.: Natural variation of radionuclide ^{137}Cs concentration in marine organisms with special reference to the effect of food habits and trophic level, Mar. Ecol. Prog. Ser., 160, 109–120, 1997.

Title Page

Abstract | Introduction

Conclusions | References

Tables | Figures

◄ | ►

Back | Close

Full Screen / Esc

Printer-friendly Version

Interactive Discussion

Kawamura, H., Kobayashi, T., Furuno, A., Ishikawa, Y., Nakayama, T., Shima, S., and Awaji, T.: Preliminary numerical experiments on oceanic dispersion of ^{131}I and ^{137}Cs discharged into the ocean because of the Fukushima Daiichi nuclear power plant disaster, J. Nucl. Sci. Technol., 48, 1349–1356, 2011.

Kempe, S. and Nies, H.: Chernobyl nuclide record from a North Sea sediment trap, Nature, 329, 828–831, 1987.

Kogure, T., Morimoto, K., Tamura, K., Sato, H., and Yamagishi, A.: XRD and HRTEM evidences for fixation of cesium ions in vermiculite clay, Chem. Lett., 41, 380–382, 2012.

Kusakabe, M., Ku, T.-L., Harada, K., Taguchi, K., and Tsunogai, S.: Chernobyl radioactivity found in mid-water sediment interceptors in the N Pacific and Bering Sea, Geophys. Res. Lett., 15, 44–47, 1988.

Masumoto, Y., Miyazawa, Y., Tsumune, D., Kobayashi, T., Estournel, C., Marsaleiz, P., Lanerolle, L., Mehra, A., and Garraffo, Z. D.: Oceanic dispersion simulation of cesium 137 from Fukushima Daiichi nuclear power plant, Elements, 8, 207–212, 2012.

Miyazawa, Y., Masumoto, Y., Varlamov, S. M., Miyama, T., Takigawa, M., Honda, M., and Saino, T.: Inverse estimation of source parameters of oceanic radioactivity dispersion models associated with the Fukushima accident, Biogeosciences Discuss., 9, 13783–13816, doi:10.5194/bgd-9-13783-2012, 2012.

Morino, Y., Ohara, T., and Nishizawa, M.: Atmospheric behavior, deposition, and budget of radioactive materials from the Fukushima Daiichi nuclear power plant in March, Geophys. Res. Lett., 38, L00G11, doi:10.1029/2011GL048689, 2011.

NERH (Nuclear Emergency Response Headquarters, Government of Japan): Report of Japanese Government to the IAEA Ministerial Conference on Nuclear Safety, – The Accident at TEPCO's Fukushima Nuclear Power Stations –, http://www.kantei.go.jp/foreign/kan/topics/201106/iaea_houkokusho_e.html, 2011.

Otosaka, S. and Kobayashi, T.: Sedimentation and remobilization of radiocesium in the coastal area of Ibaraki, 70 km south of the Fukushima Dai-ichi nuclear power plant, Environ. Monit. Assess., doi:10.1007/S10661-012-2956-7, 2012.

Qin, H., Yokoyama, Y., Fan, Q., Iwatani, H., Tanaka, K., Sakaguchi, A., Kanai, Y., Zhu, J., Onda, Y., and Takahashi, Y.: Investigation of cesium adsorption on soil and sediment samples from Fukushima prefecture by sequential extraction and EXAFS technique, Geochem. J., 46, 297–302, 2012.

Title Page

Abstract | Introduction

Conclusions | References

Tables | Figures

◄ | ►

◄ | ►

Back | Close

Full Screen / Esc

Printer-friendly Version

Interactive Discussion

Tsumune, D., Tsubono, T., Aoyama, M., and Hirose, K.: Distribution of oceanic ^{137}Cs from the Fukushima Daiichi Nuclear Power Plant simulated numerically by a regional ocean model, J. Environ. Radioact., 111, 100–108, 2011.

Whitehead, N. E., Ballestra, S., Holm, E., and Huynh-Ngoc, L.: Chernobyl radionuclides in shellfish, J. Environ. Radioact., 7, 107–121, 1988.

WHO (World Health Organization): Health hazards from radiocaesium following the Chernobyl nuclear accident, Report on a WHO working group, J. Environ. Radioact., 10, 257–259, 1989.

Fukushima-derived radiocesium in western North Pacific sediment traps

M. C. Honda et al.

Title Page

Abstract | Introduction

Conclusions | References

Tables | Figures

◄ | ►

Back | Close

Full Screen / Esc

Printer-friendly Version

Interactive Discussion

Table 1a. Specific activities and fluxes of radiocesium at (a) K2 and (b) S1. The analytical error is base on one sigma of counting statistics. Activities are decay-corrected based on middle day of each sampling period. B.D.L. is below detection limit (0.01 Bq). (B.D.L.) is below detection limit because of insufficient sample mass and activity by gamma procedures.

Station depth	Opening day	^{134}Cs activity (Bq g^{-1})	^{137}Cs activity (Bq g^{-1})	^{134}Cs/^{137}Cs	TMF (mg m^2 day^{-1})	^{134}CsFlux (mBq m^2 day^{-1})	^{134}Cs Flux (mBq m^2 day^{-1})
K2	1 Mar	B.D.L.	B.D.L.	–	35.0	–	–
500 m	13 Mar	B.D.L.	B.D.L.	–	51.2	–	–
	25 Mar	0.48 ± 0.03	0.41 ± 0.01	1.16 ± 0.07	75.4	36.2 ± 2.1	31.1 ± 0.6
	6 Apr	0.37 ± 0.04	0.35 ± 0.01	1.06 ± 0.13	55.9	20.9 ± 2.4	19.8 ± 0.8
	18 Apr	0.40 ± 0.05	0.34 ± 0.02	1.16 ± 0.15	80.0	31.9 ± 3.7	27.5 ± 1.4
	30 Apr	0.16 ± 0.05	0.16 ± 0.02	1.00 ± 0.33	33.6	5.3 ± 1.7	5.4 ± 0.6
	12 May	0.21 ± 0.06	0.19 ± 0.02	1.11 ± 0.36	23.9	4.9 ± 1.5	4.4 ± 0.6
	24 May	0.20 ± 0.05	0.20 ± 0.02	0.98 ± 0.24	61.5	12.4 ± 2.9	12.6 ± 1.0
	5 Jun	0.19 ± 0.02	0.19 ± 0.01	1.00 ± 0.14	125.6	24.3 ± 3.1	24.3 ± 1.2
	17 Jun	0.13 ± 0.02	0.12 ± 0.01	1.07 ± 0.22	166.9	20.9 ± 4.0	19.6 ± 1.4
K2	1 Mar	B.D.L.	B.D.L.		37.5		
4810 m	13 Mar	B.D.L.	B.D.L.		43.2		
	25 Mar	B.D.L.	B.D.L.		66.4		
	6 Apr	0.09 ± 0.03	0.07 ± 0.01	1.16 ± 0.49	69.6	6.1 ± 2.3	5.2 ± 0.9
	18 Apr	0.11 ± 0.04	0.11 ± 0.01	0.97 ± 0.35	43.3	4.7 ± 1.6	4.9 ± 0.6
	30 Apr	0.16 ± 0.06	0.17 ± 0.02	0.94 ± 0.39	39.9	6.3 ± 2.5	6.6 ± 0.9
	12 May	(B.D.L.)	(B.D.L.)		5.0		
	24 May	0.34 ± 0.11	0.33 ± 0.04	1.01 ± 0.37	13.3	4.5 ± 1.5	4.4 ± 0.6
	5 Jun	0.24 ± 0.04	0.22 ± 0.02	1.10 ± 0.21	79.3	18.8 ± 3.1	17.1 ± 1.5
	17 Jun	(B.D.L.)	(B.D.L.)		5.8		

Table 1b. Specific activities and fluxes of radiocesium at (a) K2 and (b) S1. The analytical error is base on one sigma of counting statistics. Activities are decay-corrected based on middle day of each sampling period. B.D.L. is below detection limit (0.01 Bq). (B.D.L.) is below detection limit because of insufficient sample mass and activity by gamma procedures.

Station depth	Opening day	^{134}Cs activity (Bq g^{-1})	^{137}Cs activity (Bq g^{-1})	^{134}Cs/^{137}Cs	TMF (mg m^2 day^{-1})	^{134}CsFlux (mBq m^2 day^{-1})	^{134}Cs Flux (mBq m^2 day^{-1})
Si 500 m	1 Mar	B.D.L.	B.D.L.	–	77.9	–	–
	13 Mar	B.D.L.	B.D.L.	–	127.4	–	–
	25 Mar	0.03 ± 0.01	0.03 ± 0.00	1.24 ± 0.44	126.3	4.4 ± 1.5	3.5 ± 0.5
	6 Apr	(B.D.L.)	(B.D.L.)		37.2		
	18 Apr	0.16 ± 0.03	0.16 ± 0.01	0.98 ± 0.20	52.3	8.3 ± 1.6	8.5 ± 0.6
	30 Apr	0.12 ± 0.05	0.11 ± 0.03	1.16 ± 0.57	24.9	3.1 ± 1.3	2.6 ± 0.6
	12 May	0.11 ± 0.05	0.10 ± 0.02	1.06 ± 0.53	26.1	2.8 ± 1.3	2.7 ± 0.5
	24 May	(B.D.L.)	(B.D.L.)		16.5		
	5 Jun	0.22 ± 0.06	0.23 ± 0.02	0.95 ± 0.27	40.5	8.9 ± 2.3	9.3 ± 0.9
	17 Jun	0.28 ± 0.05	0.21 ± 0.02	1.36 ± 0.27	27.6	7.8 ± 1.4	5.7 ± 0.5
	29 Jun	0.22 ± 0.08	0.20 ± 0.03	1.10 ± 0.43	14.6	3.2 ± 1.2	2.9 ± 0.4
	11 Jul	0.17 ± 0.06	0.18 ± 0.03	0.92 ± 0.38	15.1	2.5 ± 1.0	2.7 ± 0.4
Si 4810 m	1 Mar	B.D.L.	B.D.L.		63.0		
	13 Mar	B.D.L.	B.D.L.		170.4		
	25 Mar	B.D.L.	B.D.L.		98.2		
	6 Apr	0.09 ± 0.04	0.07 ± 0.01	1.31 ± 0.57	63.8	6.0 ± 2.3	4.5 ± 0.9
	18 Apr	0.16 ± 0.03	0.13 ± 0.01	1.25 ± 0.25	100.0	15.7 ± 2.9	12.6 ± 1.2
	30 Apr	0.22 ± 0.03	0.19 ± 0.01	1.20 ± 0.18	147.0	32.9 ± 4.4	27.3 ± 1.7
	12 May	0.19 ± 0.05	0.18 ± 0.02	1.04 ± 0.26	64.6	12.3 ± 2.9	11.9 ± 1.1
	24 May	0.14 ± 0.07	0.13 ± 0.03	1.08 ± 0.53	31.9	4.6 ± 2.1	4.3 ± 0.8
	5 Jun	0.17 ± 0.05	0.12 ± 0.02	1.37 ± 0.50	21.7	3.6 ± 1.2	2.6 ± 0.5
	17 Jun	0.24 ± 0.07	0.18 ± 0.03	1.33 ± 0.42	19.2	4.6 ± 1.3	3.4 ± 0.5
	29 Jun	0.13 ± 0.06	0.11 ± 0.02	1.19 ± 0.63	20.8	2.7 ± 1.3	2.3 ± 0.4
	11 Jul	0.19 ± 0.09	0.16 ± 0.04	1.16 ± 0.66	20.9	3.9 ± 2.0	3.3 ± 0.9

Table 2. Total radiocesium flux, average radiocesium activity, suspected ^{137}Cs inventory (see text), and removal rate of ^{137}Cs from and residence time of ^{137}Cs at surface water.

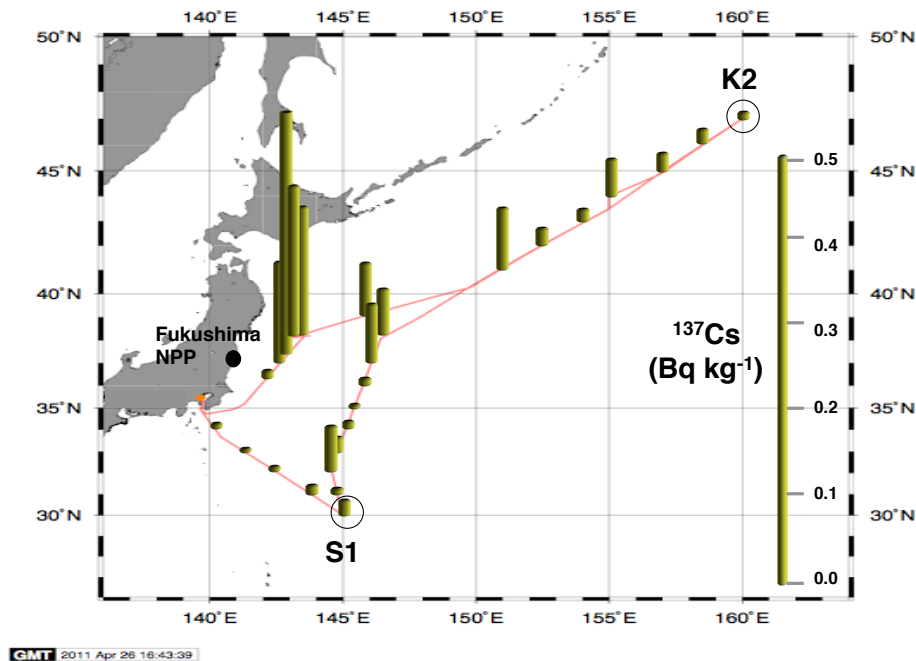|	Average ^{134}Cs activity (Bq g^{-1})	Average ^{137}Cs activity (Bq g^{-1})	Total ^{134}Cs Flux (Bq m^{-2})	Total ^{137}Cs Flux (Bq m^{-2})	Total sampling period (day)	Average ^{137}Cs Flux (mBq m^{-2} day^{-1})	^{137}Cs inventory (Bq m^{-2})	Removal rate (% yr^{-1})	Residence time (yr)
K2 500	0.27 ± 0.13	0.25 ± 0.11	1.9	1.7	96	18.1	450	1.5	68
K2 4810	0.19 ± 0.10	0.18 ± 0.10	0.5	0.5	60	7.6	450	0.6	161
Si 500	0.16 ± 0.08	0.15 ± 0.07	0.5	0.5	96	4.7	540	0.3	312
S1 4810	0.17 ± 0.05	0.14 ± 0.04	1.0	0.9	108	8.0	540	0.5	184

Fig. 1. Sediment trap location. Background is horizontal distribution of ^{137}Cs specific activity along R/V MIRAI MR11-02 cruise track in April 2011 (Honda et al., 2012).
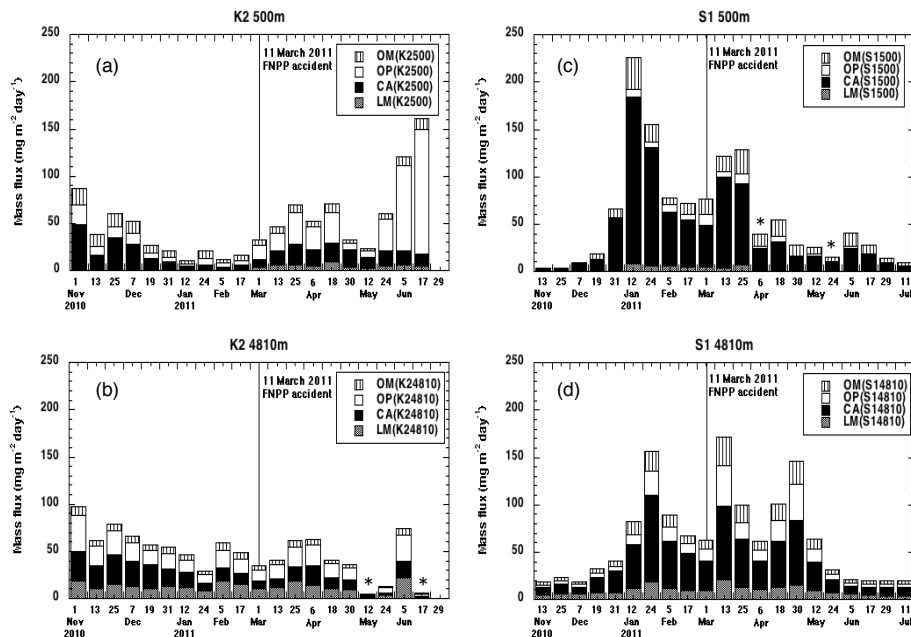
Fig. 2. Seasonal variability of sinking particles at **(a)** K2-500 m, **(b)** K2-481 m, **(c)** S1-500 m and **(d)** S1-4810 m. Chemical compositions of OM, OP, CA and LM express organic materials, biogenic opal, $CaCO_3$ and lithogenic materials, respectively. Date is opening day of respective collecting cups. Radiocesium was measured on sinking particle samples collected after 1 March 2011. From samples with asterisk, radiocesium derived from the FNPP1 accident was not detected because of insufficient sample mass.

Title Page

Abstract | Introduction

Conclusions | References

Tables | Figures

|◄ | ►|

◄ | ►

Back | Close

Full Screen / Esc

Printer-friendly Version
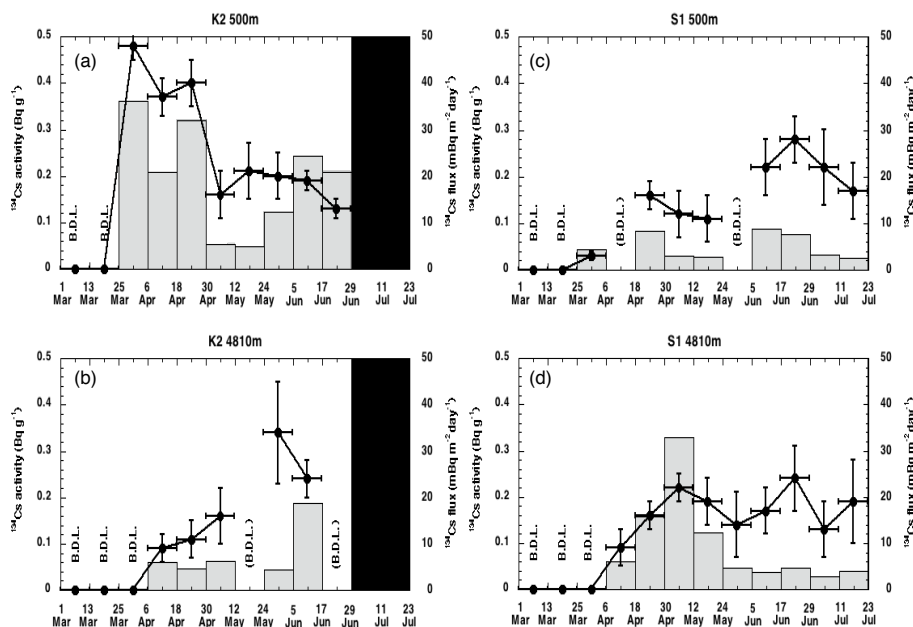
Interactive Discussion

Fig. 3. Variability of ^{134}Cs specific activity (line graph) and ^{134}Cs flux at **(a)** K2-500 m o, **(b)** K2-4810 m, **(c)** S1-500 m and **(d)** S1-4810 m. B.D.L. is below detection limit. B.D.L. in parenthesis is below detection limit likely caused by insufficient sample mass and radiocesium for gamma ray analysis.

Title Page

Abstract | Introduction

Conclusions | References

Tables | Figures

|◄ | ►|

◄ | ►

Back | Close

Full Screen / Esc